Mechanical Behavior of Nanocrystalline Au Films as a Function of Strain Rate and Film Thickness

N. Karanjgaokar[1], K. Jonnalagadda[2], I. Chasiotis[2], D. Peroulis[3], and H. Hsu[3]
[1]Mechanical Science and Eng., University of Illinois at Urbana-Champaign, Urbana, IL 61801
[2]Aerospace Engineering, University of Illinois at Urbana-Champaign, Urbana, IL 61801, USA.
[3]School of Electrical and Computer Engineering, Purdue University, IN 47907, USA.

ABSTRACT

Gold thin films are widely employed as structural and electrical contact elements in RF-MEMS. A comprehensive experimental investigation was carried out by uniaxial tension experiments to extract the strain rate dependent mechanical behavior of nanocrystalline Au films in the range of 10^{-6} - 10^{-1} s^{-1}. Full-field strain measurements were obtained with the aid of a fine speckle pattern (1 μm particle size) that assisted the use of digital image correlation. Our microscale tension experiments on Au films at different strain rates and for 0.83 μm and 1.76 μm thick specimens showed a clear monotonic increase in the elastic limit (≤ 640 MPa), yield stress (≤ 901 MPa), and ultimate tensile strength (≤ 938 MPa) with increasing loading rate. The nanocrystalline films demonstrated very large strengths and ductility: at the slowest strain rate, the ultimate failure strain was as high as 7%. Finally, the elastic modulus was not affected by the strain rate, E= 69.1± 2.1 GPa, and demonstrated small scatter across all strain rates.

1. INTRODUCTION

Gold (Au) films are used in RF-MEMS devices, such as tunable filters, micro-switches, etc. because of gold's chemical inertness, low processing temperature, and outstanding electrical conductivity. However, the reliability and performance of Au devices are highly dependent on the mechanical properties of Au films. The latter may depend on film thickness, grain size, and texture, which are largely determined by the fabrication method.

To date, the mechanical behavior of Au thin films has been obtained by a number of techniques, such as membrane deflection [1], tensile testing [2-4], nanoindentation [5-6], beam bending [7] and bulge testing [8]. The authors in [1] have reported strong size dependence of the yield stress in Au films that were thinner than 1 μm. It was reported that the reduction in the number of grains across the film could cause geometrical constraints to dislocation motion [1,9]. However; the authors in [6] have attributed the change in the mechanical behavior of films with different thicknesses to the Hall-Petch effect. In terms of RF- MEMS devices, reduction of the grain size would directly result in larger yield strains and therefore, larger operation stresses. Thus, small grain size (e.g. nanocrystalline Au) is preferable in such applications.

On the other hand, RF- MEMS operate in a broad range of frequencies, depending on the method of actuation and the application requirements. For this reason it is important to understand the strain rate dependence of the mechanical response of Au films. To put it in simple terms, quantities taken as material properties, such as yield strength and elastic (proportional) limit do not have a unique value for a metal, but they may strongly depend on the rate of loading. The authors in [3] have reported that the mechanical properties of fine grained gold films exhibited increased sensitivity to strain rate. The authors in [4] have investigated the effect of strain rate on yield, ductility, and strength of Au films with specific thicknesses, and average grain sizes 100 - 200 nm. In the current study, full-field strain measurements were obtained to determine the true strain in the specimens and thus, eliminate the measurement uncertainties that are inherent in crosshead displacement measurement methods [2-4]. This study also investigates the thickness dependence of yield stress, ultimate strength, elastic limit, and ductility, for three different thicknesses of nanocrystalline Au, in the range of strain rates 10^{-6} to 10^{-1} s^{-1}.

2. SPECIMEN FABRICATION AND EXPERIMENTAL PROCEDURES

In this paper, 100 μm wide tensile Au specimens, shown in Figure 1, were fabricated by RF sputter deposition on an oxidized silicon wafer at Purdue University. A 5000 Å layer of thermal oxide was grown on double side polished high-resistivity silicon wafers in a furnace at 1100°C in the presence of steam for 45-50 min. The SiO_2 layer was patterned and etched by S1813/S1827 photoresist to form a trench. The Si, exposed by this process, was later removed by micromachining to release the test structures. The SiO_2 was wet etched for approximately 24 minutes by using a Buffered Oxide Etch (BOE) solution. The photoresist was then removed by Acetone followed by Oxygen plasma etching. RF sputtering was used to deposit approximately 200 Å (2 min, 200 W, 4.2 mTorr, 40 sccm Ar) of Ti followed by Au to produce three Au thicknesses (0.5 μm, 0.83 μm and 1.76 μm). The Au/Ti on the test structure was patterned and etched by S1827 photoresist. Then, Au was etched by Transene TFA etchant, while Ti was etched by $HF:H_2O_2$:DI at a ratio 1:1:20. The test structures were released using XeF_2 in the Xactix™ XeF_2 etcher at etching conditions of 3 Torr, and 30×15 sec cycles.

A very fine speckle pattern was deposited on the top surface of the specimens using silicon particles, less than 1 μm in diameter, to enable the use of digital image correlation (DIC) so that full-field displacement measurements could be performed after tensile testing [10,11].

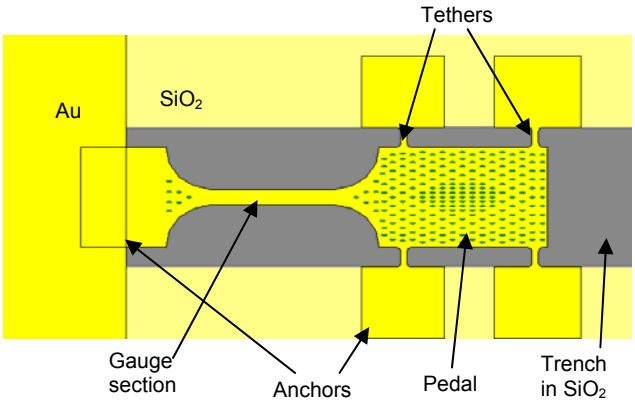

Figure 1. Schematic of a 100 μm microscale tension Au specimen. The pattern of elliptical etch-holes was developed to avoid specimen failure at the grips.

The 100-μm wide microscale tension Au specimens were tested at different loading rates by a custom built tensile testing apparatus described in [10,11]. A static membrane-based load cell was used at the lower loading rates (10^{-6} s^{-1} to 10^{-3} s^{-1}), while a dynamic load cell was employed for testing at the higher loading rates (10^{-3} s^{-1} to 10^{-1} s^{-1}). At all loading rates, a 60 μm travel length preloaded piezoelectric stack actuator was used.

The microscale tension experiments were conducted under an optical microscope at magnification 200×. Very careful specimen alignment was required during these experiments as there was no ability for correction of the specimen focus during the fast experiments. A 15 fps CCD camera captured 1024×768 resolution images at the lower rates (10^{-6} s^{-1} to 10^{-3} s^{-1}), while 512×512 resolution images were captured at 1000-2000 fps by a high speed camera for the higher strain rates (10^{-3} s^{-1} to 10^{-1} s^{-1}). During each experiment, the specimen was loaded well within the elastic limit, unloaded to the original pre-load, and then reloaded to the failure. Tests conducted at 10^{-3} s^{-1} rate by using both the static and dynamic load cells provided nearly identical results.

The DIC algorithm was employed to obtain full-field strain measurements from the specimens as a function of time. The DIC method calculates the displacement fields by defining a correlation coefficient as a function of a kinematic transformation relating the deformed to the undeformed sample geometry. The displacements are parameters in this mapping, and they are determined by a (nonlinear, multiple degree of freedom) optimization of a correlation coefficient. The displacement fields obtained via DIC were subsequently used to compute full-field

strains by a MATLAB routine. The special value of this technique lies with the sub-pixel resolution in full-field strains, which allows to monitor phenomena such as crack nucleation. The strain in each specimen was calculated by averaging the full-field strains. Consequently, the measurement uncertainty is quite small compared to two-point displacement measurements generally employed in tensile testing at these scales [2-4]. The method employed here has been shown to provide displacement accuracy as good as 23 nm in the case of uniform fields [12].

The load cell data used to calculate the engineering stress at a given instant and the stress and strain were matched in the temporal domain to obtain the stress-strain curves, Figure 2. The unloading part of the loading cycle was used to calculate the elastic modulus. The elastic limit was calculated from the stress-strain curves, and the yield stress was calculated by using the 0.2 % strain rule.

3. RESULTS AND DISCUSSION

Two different dies for each of the 0.83 μm and 1.76 μm film thicknesses were tested at loading rates 10^{-6} -10^{-1} s^{-1}. The results are presented together, but only a slight variation in properties was observed between specimens of the same thickness. Moreover, the texture and the grain size were measured by X-Ray diffraction. Irrespective of their thickness, all films had strong <111> texture and average grain size ~ 40 nm, see Table 1. It should be noted that the grain sizes are reported in grain growth direction.

Table 1: X-Ray diffraction results for different thicknesses of Au films

Material	Film thickness (μm)	Grain size (nm)	Lattice constant (nm)
Au	0.50	40.5	0.40794
	0.83	44.4	0.40909
	1.76	38.1	0.40955

The variation in the mechanical properties for different thicknesses computed from Figures 2(a-c) is shown in Figures 3(a-c). As expected, the elastic modulus for the two thickest films was rate independent with an average value of E= 69.1±2.1 GPa, which is comparable to the value of modulus of bulk Au, E= 78 GPa. The yield strength, elastic limit, and ultimate strength, however, increased monotonically with increasing strain rate, while the ultimate failure strain monotonically decreased. These results were found to be in agreement with literature on fine-grained Au films [3-4]. Similar rate dependent behavior has been reported for nanocrystalline Ni films [13].

It was noticed that the ductility of 0.83 μm thick films was between 2.2-2.8% for rates 10^{-1}-10^{-4} s^{-1} but it suddenly increased to 5.8-7.0% at 10^{-5} s^{-1}. This indicates that at rates slower than 10^{-5} s^{-1}, the creep rate at the maximum strength is comparable, or faster than, to the applied cross-head displacement rate. Therefore, the particular Au films are prone to significant creep. A similar behavior was exhibited by the 1.76 μm films at rates below 10^{-5} s^{-1}. Since all film thicknesses had similar grain size (~40 nm) and the same texture <111>, any differences in the mechanical response of films with different thickness is owed to constraints imposed by the film thickness. Such size dependence of Au film properties has been reported before [1]. In the present measurements, the elastic limit, yield stress, and ultimate strength of 0.83-μm films were generally higher than those of 1.76-μm films. It is also noteworthy that the mechanism responsible for increased ductility in 0.83-μm films was observed at a rate (10^{-5} s^{-1}) that was one order of magnitude faster than the corresponding rate (10^{-6} s^{-1}) for 1.76-μm thick films. Otherwise, the overall mechanical response of the 1.76-μm films agreed with that at a rate order of magnitude faster for the 0.83-μm films. It can therefore be concluded that thicker Au films would be less prone to creep. Although, there are very limited data available for 0.5 μm films, a comparison at 10^{-1} s^{-1} strain rate shows that the ductility increased with decreasing film thickness, from 1.76 to 0.5 μm.

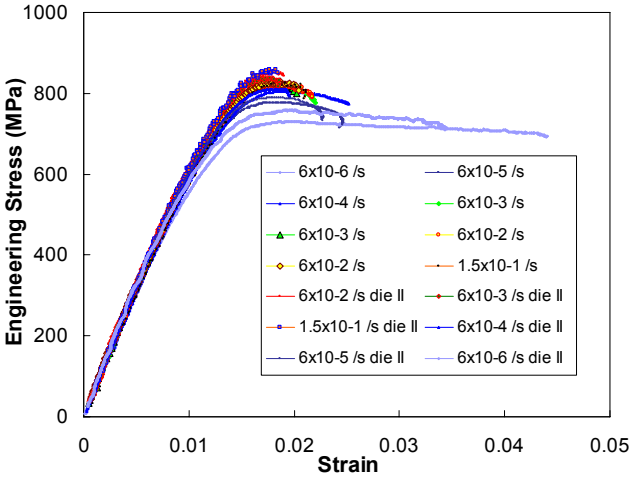

(a)

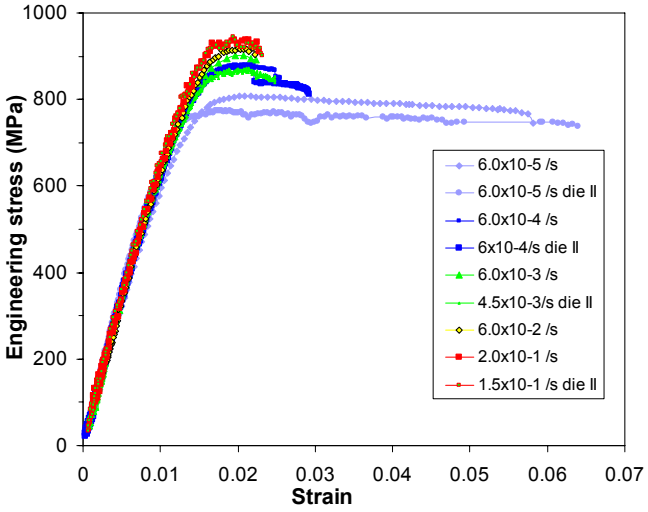

(b)

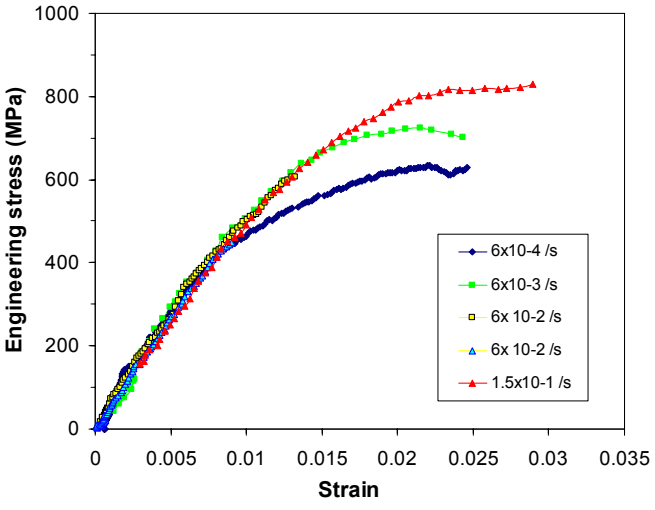

(c)

Figure 2. Stress-strain curves of Au films for different strain rates, for **(a)** 1.76-μm, **(b)** 0.83-μm, and **(c)** 0.5-μm thick nanocrystalline Au films.

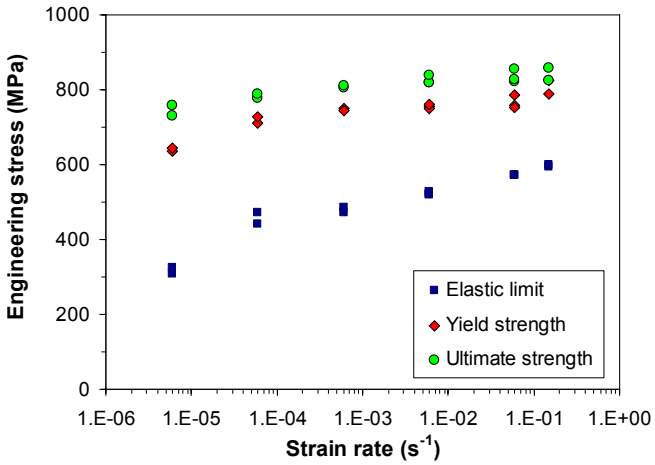

(a)

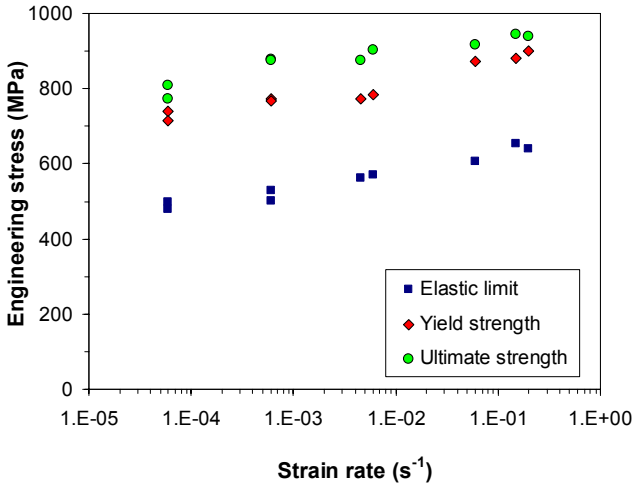

(b)

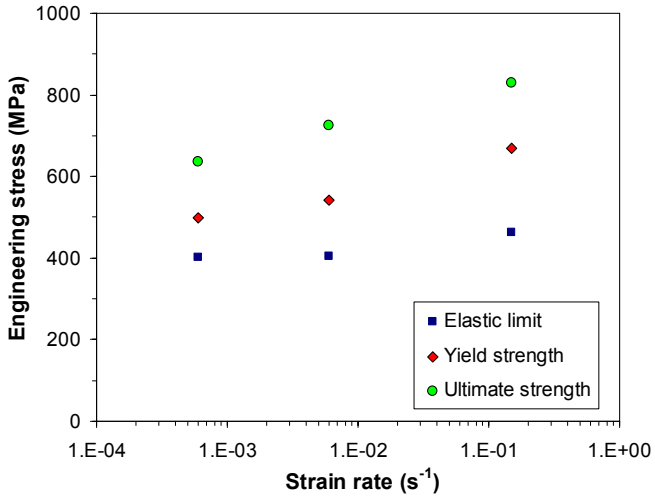

(c)

Figure 3. Ultimate strength, yield strength and elastic limit as a function of strain rate for **(a)** 1.76-μm **(b)** 0.83-μm, and **(c)** 0.5-μm thick nanocrystalline Au films.

However, the mechanical response of 0.5 μm films was not entirely consistent with that of the thicker films. The 0.5-μm Au films had lower elastic modulus with an average value of 53 GPa. For this thickness, film failure occurred for some specimens before the elastic limit. The lower modulus values can be explained in terms of the high surface roughness, Figure 4(a) of the thinnest films. As reported before [14], high surface roughness results in increased effective tensile and bending compliance in conjunction with an uncertainty in the average film thickness. Further analysis of this behavior will be part of future work. However, irrespective of the lower modulus, the thinnest specimens demonstrated significant rate sensitivity too. These initial experiments for this thickness suggested that the yield strength, elastic limit, and ultimate tensile strength of specimens that failed at stresses larger than the average elastic limit, increased monotonically with increasing strain rate. The failure strain was similar at all rates potentially due to large critical surface flaws. Further work is required to better understand this behavior of the 0.5 μm Au films.

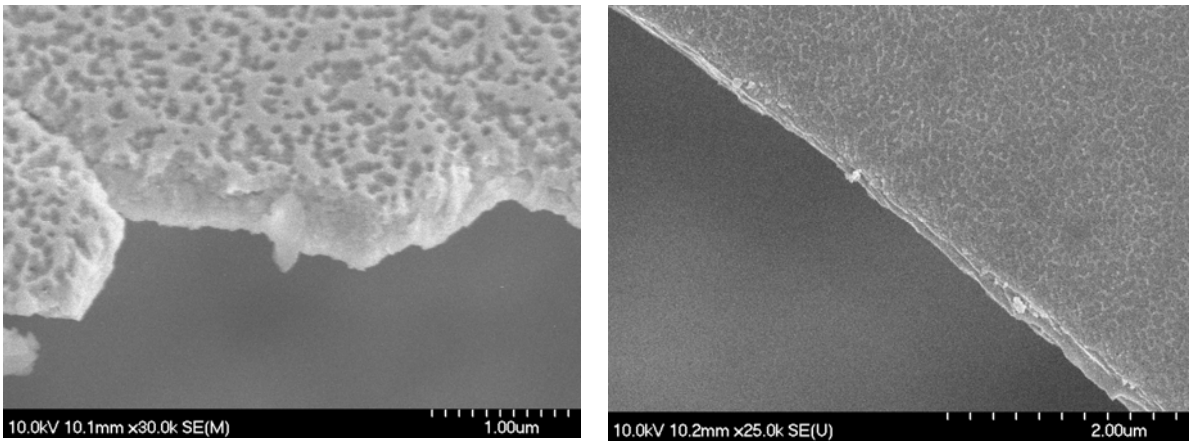

(a) **(b)**

Figure 4. Fracture cross-sections for **(a)** 0.5-μm Au film loaded at 10^{-3} s^{-1} and **(b)** 0.83-μm Au film loaded at 10^{-3} s^{-1}. Notice the large surface roughness on the top surface and the serrated fracture, normal to the applied load, in film **(a)**, contrary to the ductile fracture due to shear localization in film **(b)** where the failure cross-section was 45° with respect to the applied load.

4. CONCLUSIONS

In this paper, the rate dependence of the elastic limit, yield strength, and ultimate strength of nanocrystalline Au films were investigated for the first time for three different thicknesses and at strain rates from 10^{-6} - 10^{-1} s^{-1}. It was shown that all the aforementioned properties monotonically increased with increasing strain rate for all of the three thicknesses. For 0.83-μm and 1.76-μm thick Au films, the ultimate failure strain decreased monotonically with increasing strain rates, but below a certain threshold strain rate, the ductility increased drastically, pointing to enhanced creep at the particular or smaller strain rates. A distinct thickness dependence of the material ductility and elastic limit was shown for 0.83 μm and 1.76 μm thicknesses: The mechanical response of films with the higher thickness at a particular rate qualitatively and, in some cases, quantitatively agreed with that for the lower film thickness at an order of magnitude faster strain rate. The elastic moduli of the 0.83 μm and 1.76 μm films were independent of strain rate which provides further confidence in our experimental method. Finally, all inelastic properties for all three thicknesses of nanocrystalline Au were shown to be significantly higher than those reported in literature before, which is a consequence of the small grain size (40 nm) which may be explained according to the Hall-Petch effect.

5. ACKNOWLEDGEMENTS

The authors acknowledge the support by the DARPA MEMS/NEMS Science & Technology (S&T) Fundamentals Grant # HR0011-06-1-0046 with Dr. D. Polla as the Program Manager, and Dr. A. Cangellaris as the Director of the Beckman Center for Advancement of MEMS/NEMS VLSI (IMPACT).

6. REFERENCES

[1] Espinosa, H.D. Prorok, B. C. ”Size effects on the mechanical behavior of gold thin films,” Journal of Materials Science 38 pp. 4125 – 4128 2003.

[2] Emery R.D., Povirk G.L. “Tensile behavior of free-standing gold films. Part I: Coarse-grained films,” Acta Materialia 51 pp. 2067–2078 2003.

[3] Emery R.D., Povirk G.L. “Tensile behavior of free-standing gold films. Part II: Fine-grained films,” Acta Materialia 51 pp. 2079–2087 2003.

[4] Chasiotis I., Bateson C., Timpano K. , McCarty A.S., Barker N.S., Stanec J.R. “Strain rate effects on the mechanical behavior of nanocrystalline Au films,” Thin Solid Films 515 pp. 3183–3189 2007.

[5] Volinsky A. A., Moody N. R., Gerberich W. W. “Nanoindentation of Au and Pt/Cu thin films at elevated temperatures,” Journal of Material Research Vol. 19 No. 9 pp. 2650-2657 2004.

[6] Cao Y., Allameh S., Nankivil D., Sethiaraj S., Otiti T., Soboyejo W. “Nanoindentation measurements of the mechanical properties of polycrystalline Au and Ag thin films on silicon substrates: Effects of grain size and film thickness,” Materials Science and Engineering A 427 pp. 232–240 2006.

[7] Baeka C., Kima Y., Ahnb Y., Kimc Y. “Measurement of the mechanical properties of electroplated gold thin films using micromachined beam structures,” Sensors and Actuators A 117 pp. 17–27 2005.

[8] Li.Y., Cima M.J. “Bulge test on free standing gold thin films,” Thin Films - Stresses and Mechanical Properties X. Material Research Society Symposium Proceedings Vol.795 p 437-42 2004.

[9] Arzt E. “Size effects in materials due to microstructural and dimensional constraints: A Comparative Review,” Acta materialia 46 16 pp. 5611-5626 1998.

[10] Cho S.W., Chasiotis I. “Elastic Properties and Representative Volume Element of Polycrystalline Silicon for MEMS,” Experimental Mechanics 47 pp. 37–49 2007.

[11] Chasiotis, I., Knauss, W.G., “A New Microtensile Tester for the Study of MEMS Materials with the aid of Atomic Force Microscopy”, Experimental Mechanics 42 (1), pp. 51-57 2002.

[12] Naraghi, M., Chasiotis, I., Dzenis, Y., Wen, Y., Kahn, H., “Novel Method for Mechanical Characterization of Polymeric Nanofibers”, Review of Scientific Instruments 78, pp. 085108-1-085108-7 2007.

[13] Schwaiger R., Moser B., Dao M., Chollacoop N., Suresh S. “Some critical experiments on the strain-rate sensitivity of nanocrystalline nickel,” Acta Materialia 51 pp. 5159–5172 2003.

[14] Chasiotis I., Knauss W. G. “Mechanical properties of thin polysilicon films by means of probe microscopy,” Part of the SPIE Conference on Materials and Device Characterization in Micromachining. SPIE Vol. 3512 pp. 66-75 Santa Clara, California September 1998.